# BLIND RANGES, FREQUENCIES AND DOAS ESTIMATION FOR NEAR FIELD SOURCES

*Ke Deng, Qinye Yin, Huiming Wang*

Institute of Information Engineering, School of Electronics and Information Engineering, Xi'an Jiaotong University, Xi'an 710049, China
E-mail: anthony.deng@gmail.com, qyyin@mail.xjtu.edu.cn

## ABSTRACT

Two novel algorithms are proposed for ranges, frequencies and direction-of-arrivals (DOAs) estimation of the narrow-band near field sources. By exploiting the time-domain and space-domain correlations of impinging signals jointly, we can identify $2p$ independent sources and estimate 3 groups of parameters with a uniformly linear array (ULA) of $2p+1$ elements, being double of the conventional methods. In addition, the peak search and pairing operations, needed in most algorithms for near field sources, can be omitted completely in our methods. Simulation results show that our two ESPRIT-based methods provide the improved performance over conventional ones based on the second-order statistics.

*Index Terms* — Array signal processing, Direction of arrival estimation, Frequency estimation, Parameter estimation

## 1. INTRODUCTION

Lots of researches on array processing were focused on the far-field signals. Nevertheless, the far-field assumption does not holds in many scenarios. In these cases, the steering vectors are characterized by not only the impinging DOAs, but the ranges of the sources as well. Then, the accurate depiction of the space signature of the signals allows for the joint estimation.

In the conventional near-field signal processing, the number of identifiable sources is much fewer than that in far-field scenarios. For example, a ULA with $2p+1$ elements can identify $2p$ sources in far-field scenarios, but only $p$ sources in the near-field ones for most proposed algorithms [1-2]. The number of identifiable sources of the near-field signals is only the half of the far-field signals. The algorithms in [3-4] can estimate more sources, but they have some constraints on the sources' frequencies.

In addition, the parameters in the near-field scenarios include range, frequency and DOA (Direction-Of-Arrival), where two problems exist: the peak search and parameter pairing operations. Some algorithms based on the MUSIC method need the time-consuming peak search. Although algorithms based on the ESPRIT method or matrix-pencil theory can estimate the parameters without the search operation, they usually need the parameter pairing operation too.

In this paper, two novel DOA, frequency and range estimation algorithms are proposed for narrow-band near-field signals, which exploit both the space-domain and time-domain correlations. As a result, they can identify $2p$ or $2p-1$ sources with a ULA of $2p+1$ elements, being double of the most conventional ones using the second order statistics. In addition, one of our algorithms does not need the peak search and pair operations any more. Besides them, its computational burden is comparable with those based on the second-order statistics ones, for it only needs the same number of snapshots as the other second-order statistics ones. Simulation results show that both algorithms provide better performance than conventional ones.

* Partially supported by the National Natural Science Foundation of China(No. 60502022, 60572046, 60772095), the National Natural Science Foundation of Shaanxi(No. 2005F25) and the National Hi-Tech Research and Development Program of China(No. 2006AA01Z220).

## 2. SYSTEM MODEL

Consider a ULA having $L=2p+1$ elements with interelement spacing $d$, which is shown in Fig. 1, where the array center is designated as the phrase reference point and the origin of the coordinate system. Then, the signal received by the $l$-th sensor is expressed as

$$x_l(t)=\sum_{m=1}^{M} s_m(t)e^{j\tau_{lm}}+n_l(t) \qquad -p\le l\le p \tag{1}$$

where $s_m(t)$ denotes the $m$-th impinging signal, $n_l(t)$ is the additive white Gaussian noise (AWGN), and $\tau_{lm}$ is the delay of the $m$-th impinging signal propagation time difference between sensor "0" and sensor $l$ given by [1-2]

$$\tau_{lm}=\frac{2\pi r_m}{\lambda}\left(\sqrt{1+(\frac{ld}{r_m})^2-\frac{2ld\sin(\theta_m)}{r_m}}-1\right) \tag{2}$$

where $r_m$ and $\theta_m$ are the range and DOA of source $m$, respectively, and $\lambda$ denotes the signal wavelength. Obviously, $\tau_{lm}$ is not a linear function of $r_m$ and $\theta_m$ any more, and the DOA estimation methods in far-field scenarios are not adequate for this context. To work out this problem, a good approximation of $\tau_{lm}$, proposed by Fresnel, which exploits its second Tylor expansion, is expressed as

$$\tau_{lm}=\omega_m l+\phi_m l^2+O(\frac{d^2}{r_m^2}) \tag{3}$$

where $O(\frac{d^2}{r_m^2})$ corresponds to the terms of order greater or equal to $\frac{d^2}{r_m^2}$ neglected here, $\omega_m$ and $\phi_m$ are given by

$$\omega_m=-\frac{2\pi d\sin(\theta_m)}{\lambda} \tag{4}$$

$$\phi_m=\frac{\pi d^2\cos^2(\theta_m)}{\lambda r_m} \tag{5}$$

By exploiting the above approximation, $x_l(t)$ in (1) can be expressed as

$$x_l(t) = \sum_{m=1}^{M} s_m(t) e^{j(\omega_m l + \phi_m l^2)} + n_l(t) \tag{6}$$

Throughout the rest of this paper, the following hypotheses are assumed to be hold:

$\mathcal{H}1$: The source signals $s_m(t)$, $m = 1, 2, \ldots, M$ are mutually independent signals. They are narrow-band and stationary processes.

$\mathcal{H}2$: The additive noises, $n_l(t)$, $l = -p, \ldots, p$ are independent and zero-mean Gaussian processes with covariance $\sigma^2$, and are independent of the source signals.

$\mathcal{H}3$: The impinging DOAs of the sources are not equal, i.e., $\theta_i \neq \theta_j$ for $i \neq j$.

$\mathcal{H}4$: The interelement spacing of the array is $d \leq \frac{\lambda}{4}$; Additionally, the number of sources is $M \leq 2p$.

## 3. BLIND ESTIMATION ALGORITHM

### 3.1 Algorithm A

According to $\mathcal{H}1$ and $\mathcal{H}2$ in section 2, a set of space-domain correlation variables can be defined as:

$$\begin{aligned} r_{-l-1,-l}(\tau) &= E\{x_{-l-1}(t+\tau) x^*_{-l}(t)\} \\ &= \sum_{m=1}^{M} r_{sm}(\tau) e^{j(-\omega_m + \phi_m)} e^{2jl\phi_m} \\ &= \sum_{m=1}^{M} r_{sm}(0) e^{j(2\pi f_m \tau - \omega_m + \phi_m)} e^{2jl\phi_m} \end{aligned} \tag{7}$$

where $r_{sm}(\tau) \triangleq E\{s_m(t+\tau) s^*_m(t)\} = r_{sm}(0) e^{j2\pi f_m \tau}$; $s_m(t)$ is a narrow-band signal and $f_m$ is its frequency and $\delta(\cdot)$ is the Dirac function.

Similarly,

$$\begin{aligned} r_{l+1,l}(\tau) &= E\{x_{l+1}(t+\tau) x^*_l(t)\} \\ &= \sum_{m=1}^{M} r_{sm}(0) e^{j(2\pi f_m \tau + \omega_m + \phi_m)} e^{2jl\phi_m} \end{aligned} \tag{8}$$

Concatenating $r_{-l-1,-l}(\tau)$ and $r_{l+1,l}(\tau)$ where $l = -p, -p+1, \ldots, p-1$, we can construct two vectors $\mathbf{r}_1(\tau)$, $\mathbf{r}_2(\tau)$ with length $2p$. They are

$$\mathbf{r}_1(\tau) = [r_{p-1,p}(\tau), \ldots, r_{-1,0}(\tau), \ldots, r_{-p,-p+1}(\tau)]^T \tag{9}$$

$$\mathbf{r}_2(\tau) = [r_{-p+1,-p}(\tau), \ldots, r_{1,0}(\tau), \ldots, r_{p,p-1}(\tau)]^T \tag{10}$$

Alternative forms for (9)(10) are

$$\mathbf{r}_1(\tau) = \mathbf{B}\mathbf{\Phi}\mathbf{\Omega}^* \mathbf{r}_s(\tau) \tag{11}$$

$$\mathbf{r}_2(\tau) = \mathbf{B}\mathbf{\Phi}\mathbf{\Omega} \mathbf{r}_s(\tau) \tag{12}$$

where

$$\begin{aligned} \mathbf{B} &= [\,\mathbf{b}(\phi_1) \quad \ldots \quad \mathbf{b}(\phi_M)\,] \qquad 2p \times M \\ \mathbf{b}(\phi_m) &= [\,e^{-2jp\phi_m} \quad e^{-2j(p-1)\phi_m} \quad \ldots \quad e^{2j(p-1)\phi_m}\,]^T \\ \mathbf{r}_s(\tau) &= [\,e^{j2\pi f_1 \tau} r_{s1}(0) \quad \ldots \quad e^{j2\pi f_M \tau} r_{sM}(0)\,]^T \\ \mathbf{\Omega} &= \mathrm{diag}\{e^{j\omega_1}, e^{j\omega_2}, \ldots, e^{j\omega_M}\} \\ \mathbf{\Phi} &= \mathrm{diag}\{e^{j\phi_1}, e^{j\phi_2}, \ldots, e^{j\phi_M}\} \end{aligned}$$

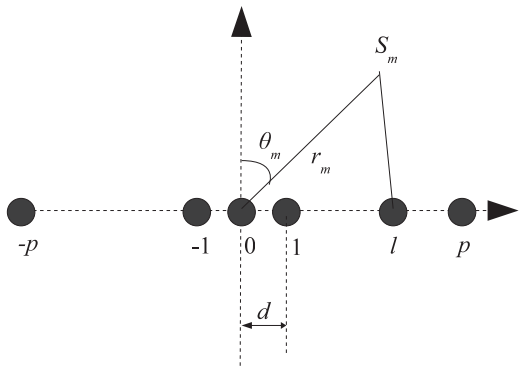


Fig. 1 The system model of near field scenarios

By sampling $\mathbf{r}_1(\tau)$ and $\mathbf{r}_2(\tau)$ uniformly at $N$ ($N > M$) lags $\tau_n$ ($\tau_n = T_s, 2T_s, \ldots, NT_s$), the "pseudo snapshots" can be collected as follows:

$$\mathbf{R_1} = [\,\mathbf{r}_1(T_s) \quad \mathbf{r}_1(2T_s) \quad \ldots \quad \mathbf{r}_1(NT_s)\,] \tag{13}$$

$$\mathbf{R_2} = [\,\mathbf{r}_2(T_s) \quad \mathbf{r}_2(2T_s) \quad \ldots \quad \mathbf{r}_2(NT_s)\,] \tag{14}$$

And also we have

$$\mathbf{R_1} = \mathbf{B}\mathbf{\Phi}\mathbf{\Omega}^* \mathbf{R}_s \tag{15}$$

$$\mathbf{R_2} = \mathbf{B}\mathbf{\Phi}\mathbf{\Omega} \mathbf{R}_s \tag{16}$$

where $\mathbf{R}_1$ and $\mathbf{R}_2$ are with dimensions $2p \times N$ and

$$\mathbf{R}_s = \begin{bmatrix} e^{j2\pi f_1 T_s} r_{s1}(0) & e^{j4\pi f_1 T_s} r_{s1}(0) & \ldots & e^{j2N\pi f_1 T_s} r_{s1}(0) \\ e^{j2\pi f_2 T_s} r_{s2}(0) & e^{j4\pi f_2 T_s} r_{s2}(0) & \ldots & e^{j2N\pi f_2 T_s} r_{s2}(0) \\ \vdots & \vdots & \ddots & \vdots \\ e^{j2\pi f_M T_s} r_{sM}(0) & e^{j4\pi f_M T_s} r_{sM}(0) & \ldots & e^{j2N\pi f_M T_s} r_{sM}(0) \end{bmatrix}$$

If we define two matrices: $\mathbf{A} \triangleq \mathbf{B}\mathbf{\Phi}\mathbf{\Omega}^*$ and $\mathbf{\Psi} \triangleq (\mathbf{\Omega})^2$, (15) and (16) can be rewritten as

$$\mathbf{R}_1 = \mathbf{A}\mathbf{R}_s \tag{17}$$

$$\mathbf{R}_2 = \mathbf{A}\mathbf{\Psi}\mathbf{R}_s \tag{18}$$

(17) and (18) are basic equations of the ESPRIT method [5], therefore, $\mathbf{\Psi}$ can be estimated directly, and $\omega_1, \ldots, \omega_M$ are also calculated in a closed form. To obtain another set of parameters $\phi_1, \ldots, \phi_M$, we need obtain $\mathbf{A}$. Because An ESPRIT-like method — DOA-Matrix method [6] can estimate $\mathbf{A}$ and $\mathbf{\Psi}$ jointly in a closed form, it is exploited in this case without the need of the simultaneous diagonalization of multiple matrices.

In the DOA-Matrix method, first we define a signature matrix as

$$\mathbf{R} = \mathbf{R}_2 [\mathbf{R}_1]^- \tag{19}$$

where $[\bullet]^-$ denotes the pseudo-inverse, i.e., $\mathbf{R}_1[\mathbf{R}_1]^- = \mathbf{I}$. And we have the following lemma.

*Lemma:* If $\mathbf{A}$ is full column rank, $\mathbf{R}_s$ has no zero singular values, and $\mathbf{\Psi}$ has no equal elements on the main diagonal line, the nonzero eigen values of $\mathbf{R}$ equal to the $d$ diagonal elements of $\mathbf{\Psi}$, and corresponding eigenvectors equal to the $d$ columns of $\mathbf{A}$, i.e.

$$\mathbf{R}\mathbf{A} = \mathbf{A}\mathbf{\Psi} \tag{20}$$

The detail proof is in [6].

According to the hypotheses and the lemma, once $\mathbf{A}$ is full-column rank, both $\mathbf{\Psi}$ and $\mathbf{A}$ can be calculated by an eigen value decomposition (EVD) operation. Because $\mathbf{A}$ is with

dimensions $2p \times M$, if the number of sources $M$ is less than $2p$, $\mathbf{A}$ is full column rank and this algorithm holds.

After $\mathbf{A}$ is estimated in a closed form, it is easily to estimate $\phi_1, \ldots, \phi_M$, because every column of $\mathbf{A}$ associates one $\phi_m$ only, and what is more, the quotient of two adjacent rows is just $e^{2j\phi_m}$. Also, the least mean square method can be used in this case. Note that the $\omega_m$ and $\phi_m$ are one-to-one correspondences because they are from the same pair of eigen value and vector, i.e., the parameters are paired automatically. Obviously, the pair operation is omitted in the whole process.

The proposed method differs from not only those MUSIC-based methods which exploit the eigen vectors only and need the operation of peak searching or rooting, but also those ESPRIT-based methods which exploit eigen values only and need the pairing operations. Our method exploits both eigen values and eigen vectors, and those operations can be skipped.

To estimate the sources' frequencies $f_1, f_2, \ldots, f_M$, we perform the transpose operation for $\mathbf{R}_1$ and $\mathbf{R}_2$ in (17)(18). Then we have

$$\mathbf{R}_1^T = \mathbf{R}_s^T \mathbf{A}^T \tag{21}$$

$$\mathbf{R}_2^T = \mathbf{R}_s^T \mathbf{\Psi} \mathbf{A}^T \tag{22}$$

(21) and (22) are also the basic equations of ESPRIT method, and similarly, DOA-Matrix method can be exploited to calculate $\mathbf{\Psi}$ in a closed-form. Thus, $\mathbf{R}_s$ can be estimate in a closed form like $\mathbf{A}$ in (17) and (18). After calculated $\mathbf{R}_s$, the estimation of frequencies $f_1, f_2, \ldots, f_M$ is similar with that of $\{\phi_m\}$ from $\mathbf{A}$. It is easily observed that the quotient of two adjacent columns of row $m$ is $e^{j2\pi f_m}$ in $\mathbf{R}_s$. Thus, the least square method can also be used. Just like the estimation of $\phi_m$ and $\omega_m$, the $\phi_m$ and $f_m$ are auto paired.

Our method exploits both the space-domain and the time-domain correlations, differing from those exploiting the space-domain correlation only. Therefore, it can approximately estimate double independent sources of what other methods did.

Although more correlations are calculated in our algorithm, the most time-consuming operation is still the EVD operation. Its times are not increased and some time-consuming operations like peak searching and pairing are omitted. Our method does not increase the computational burden on a large scale, which is still comparable with the conventional ones.

### 3.2 Algorithm B

If $\mathcal{H}3$ does not hold, a problem exists in algorithm A. When two $\{\theta_m\}$ are equal or close very much, two $\{\omega_m\}$ are equal, and the corresponding $\{\phi_m\}$ can not be estimated because two calculated eigenvectors are the linear combinations of two desired one when two eigenvalues are equal. To obtain the correct signal subspace is very difficult in this case. To overcome this, another algorithm is proposed, which exploits the eigenvalues only and can avoid this shortcoming. However, the maximum number of identifiable sources decreases 1, is $2p-1$ only now.

This simple method is as follows: after estimating $\{\omega_m\}$ from the eigenvalues with algorithm A, we choose the first $2p-1$ rows and the last $2p-1$ rows of $\mathbf{R}_1$, namely $\mathbf{R}_u$ and $\mathbf{R}_d$, respectively. Because the quotient of adjacent rows in column $m$ of $\mathbf{A}$ is $e^{2j\phi_m}$, we have

$$\mathbf{R}_u = \mathbf{R}_1(1:2p-1,:) = \mathbf{A}'\mathbf{R}_s \tag{23}$$

$$\mathbf{R}_d = \mathbf{R}_1(2:2p,:) = \mathbf{A}'\mathbf{\Phi}^2\mathbf{R}_s \tag{24}$$

Table 1 The parameters of three sources

| Source no. | $r$ | $\theta(^\circ)$ | f(MHz) |
|---|---|---|---|
| 1 | $1/6\lambda$ | 15 | 20 |
| 2 | $1/4\lambda$ | 25 | 20.2 |
| 3 | $2/5\lambda$ | 35 | 19.7 |

Table 2 The performance of frequency estimation(RMSE)

| SNR | M=1 | M=2 | M=3 |
|---|---|---|---|
| -10 | 7.41e-4 | 3.74e-3 | 2.58e-2 |
| -5 | 1.48e-4 | 1.8e-3 | 3.88e-3 |
| 0 | 4.30e-5 | 1.28e-3 | 2.48e-3 |
| 5 | 1.31e-5 | 1.1e-3 | 1.41e-3 |
| 10 | 7.33e-6 | 8.94e-4 | 1.22e-3 |

where $\mathbf{A}' = \mathbf{A}(1:2p-1,:)$ is the first $2p-1$ rows of $\mathbf{A}$.

Obviously, we can estimate the $\mathbf{\Phi}$ by exploiting the ESPRIT method. Because only the eigenvalues are used in the estimating method, it can also work when two $\{\theta_m\}$ are equal. The pair operation is necessary because the $\{\omega_m\}$ and $\{\phi_m\}$ are estimated in two EVDs.

The dimensions of $\mathbf{R}_u$ and $\mathbf{R}_d$ are $(2p-1) \times M$, therefore, the maximum identifiable sources in algorithm B is $2p-1$, or the $\mathbf{A}$' is not full column rank.

Similarly, $f_1, f_2, \ldots, f_M$ can be estimated from $\mathbf{R}'_u$ and $\mathbf{R}'_d$ like in Algorithm A because two $\{\phi_m\}$ are not the same.

## 4. SIMULATIONS

In our simulations, we adopt a uniform linear array (ULA) of $L = 5$ ($p = 2$) sensors with element spacing $d = \lambda/4$. $N_t = 100$ independent Monte-Carlo simulations are performed. The performance is measured by the Root Mean Square Error (RMSE) defined as

$$\mathrm{RMSE}(\mathbf{x}) = \frac{1}{\|\mathbf{x}\|}\sqrt{\frac{1}{N_t}\sum_{i=1}^{N_t}\|\hat{\mathbf{x}}(i) - \mathbf{x}\|^2} \tag{25}$$

where $N_t$ is the number of Monte-Carlo trials, and $\| \bullet \|$ represents the Frobenius norm; and $\mathbf{x}$ represents the exact values of parameters, and $\hat{\mathbf{x}}(i)$ represents the estimated values in the $i$-th Monte-Carlo trials, respectively. $\mathbf{x}$ can be either the impinging DOAs, $\mathbf{\Theta} = \{\theta_i\}$, $i = 1, 2, \ldots$, the ranges $\mathbf{r} = \{r_i\}$, $i = 1, 2, \ldots$, or the frequencies $\mathbf{F} = \{f_i\}$, $i = 1, 2, \ldots$. In each trial, 1024 real snapshots and 30 pseudo snapshots are collected. The paramters of 3 sources are shown in Table 1, all of them are mean-zero, unit-variance and independent.

**Test Case 1— One Source:** Consider source 1 impinge the array. Three methods: MUSIC [2] and our algorithms are measured and their performances are shown in Fig. 2, where the SNR is defined as $\mathrm{SNR} = 1/\sigma^2$. With the simulation, we observe that the performances of ours are better than MUSIC methods when the SNR is relatively low because our methods can offer more noise subspace when both space and time correlations are exploited. In addition, the

time-consuming operations of peak searching and pairing are omitted in algorithm A.

**Test Case 2— Two sources:** In this case, source 1 and 2 are present. In order to measure the MUSIC method in [2], we let the number of sensors $L = 6$ while those in ours are still 5. The performance of three methods are shown in Fig. 3. From the simulations, we observe that ours obtain improved performance over MUSIC method [2] although it is equipped more elements.

**Test Case 3— Three sources:** In this case, three ($M = 3$) uncorrelated, unit-variance sources are present. MUSIC method in [2] can only identify two sources (for $p = 2$), and it can not estimate these nine parameters, while the performance of ours are shown in Fig. 4. From the simulations, we observe that the performance is still acceptable when 3 sources impinge at a 5-element ULA.

In three simulations, the performances of our two methods are very close. The reasons is that the dimensions of noise subspace in algorithm B is less than that in algorithm A, while all parameters are estimated from eigenvalues in algorithm B. Although it does not require that $\mathcal{H}3$ holds, obviously the computational burden in algorithm B is heavier than that in algorithm A for one more EVD is needed.

The performance of frequency estimation is shown in Table 2, only the performance of algorithm A is shown because the performance of two frequency estimation methods are very close. The sample frequency is 50MHz. From Table 2 we found the performance of frequency estimation is perfect even three frequencies are very close.

## 5. CONCLUSIONS

This paper proposed two near-field sources estimation algorithms by exploiting both the space-domain and the time-domain correlations where the estimated parameters include the ranges, frequencies and DOAs. As a result, they can not only identify double sources of what conventional methods offered, but also obtain better performance. Furthermore, in one of our methods the time-consuming peak search and pairing operations can be omitted completely by exploiting the eigen values and vectors simultaneously.

## REFERNCES


[1] D. Starer, A. Nehorai, ‘‘Passive localization of near-field sources by path following," *IEEE Transactions on Signal Processing*, vol. 42, no. 3, pp. 677-680, March 1994.

[2] K. Abed-Meraim, Y. Hua, A. Belouchrani, ‘‘Second-order near-field source localization: algorithm and performance analysis," *Conference Record of the Thirtieth Asilomar Conference on Signals, Systems and Computers 1996*, vol. 1, pp. 723-727, 1996.

[3] K. T. Wong, M. D. Zoltowski, ‘‘Uni-vector-sensor ESPRIT for multisource azimuth, elevation, and polarization estimation," *IEEE Transactions on Antennas and Propagation*, vol. 45, no. 10, pp.1467 - 1474, Oct. 1997.

[4] P. Tichavsky, K. T. Wong, M. D. Zoltowski, ‘‘Near-field/far-field azimuth and elevation angle estimation using a single vector hydrophone," *IEEE Transactions on Signal Processing*, vol. 49, no. 11, pp. 2498 - 2510, Nov. 2001.

[5] R. Roy, T. Kailath, ‘‘ESPRIT — Estimation of signal parameters via rotational invariance techniques," *Optical engineering*, vol. 29, no. 4, pp. 984-995, 1990.

[6] Q. Yin, R. Newcomb, L. Zou, ‘‘Estimating 2-D angle of arrival via two parallel linear array," *Proc. IEEE ICASSP'89*, vol. 3, pp. 2803-2806, 1989.

[7] L. Jin, M. Yao, Q. Yin, ‘‘Blind Closed-form Array Response Estimation in Wireless Communication," *Proc. IEEE ICASSP'99*, vol. 5, pp. 2913-2916, March 1999.


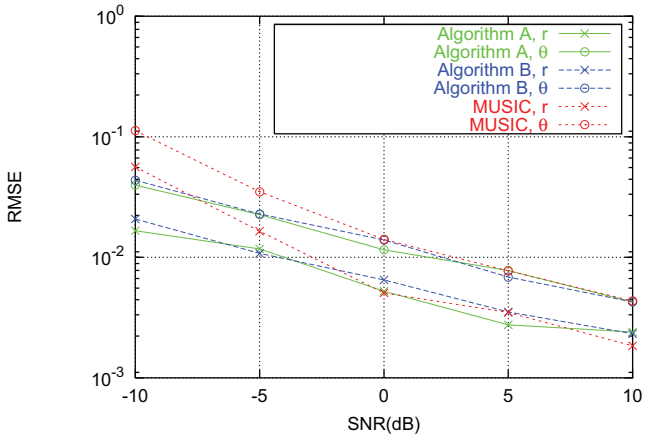


Fig. 2 The performances when $M = 1$

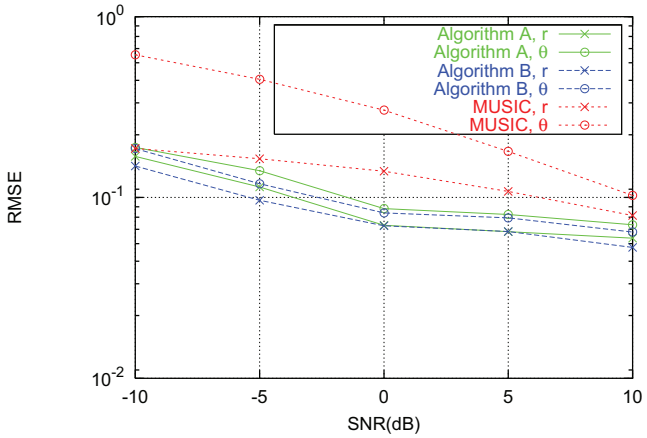


Fig. 3 The performances when $M = 2$

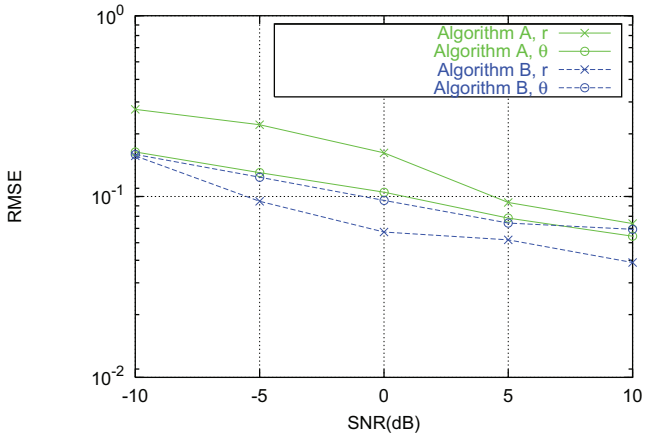


Fig. 4 The performances when $M = 3$